RevMexAA (Serie de Conferencias), **7**, 65–72 (1998)

SELF-CONSISTENT STAR FORMATION HISTORIES OF DWARF IRREGULAR GALAXIES

E. D. Skillman, R. C. Dohm-Palmer, and H. A. Kobulnicky

Astronomy Department, University of Minnesota, Minneapolis, MN 55455, USA;
skillman@zon.spa.umn.edu

RESUMEN

Usando la fotometría de las estrellas resueltas en las galaxias irregulares enanas Sextans A y la enana Pegaso tomada por WFPC2 en el *Telescopio Espacial Hubble* hemos construido diagramas color-magnitud en V e I a un límite de 26 en V. Usamos las estrellas azules con que están quemando el núcleo de helio como un indicio de la tasa de formación estelar durante los pasados 600 Myr en ambas galaxias. Mientras que Sextans A muestra un índice de formación estelar relativamente alto durante este período, la enana Pegaso ha estado relativamente inactiva. También comparamos la abundancia de la materia interestelar obtenida de observaciones de regiones H II, usando el telescopio de 3.5-m en Calar Alto. Encontramos que el medio interestelar en la enana Pegaso muestra un cociente N/O relativamente alto, mientras que Sextans A muestra un cociente N/O relativamente bajo. Estos resultados son consistentes con la hipótesis de que la producción de oxígeno está dominada por estrellas muy masivas, mientras que la producción de nitrógeno está dominada por estrellas de masas bajas e intermedias. Por lo tanto, la historia de la formación estelar como está inscrita en las estrellas, es consistente con la historia de formación de estrellas deducida de las abundancias de la materia interestelar.

ABSTRACT

Using *Hubble Space Telescope*, WFPC2 photometry of the resolved stars in the nearby dwarf irregular galaxies Sextans A and the Pegasus dwarf, we have constructed color-magnitude diagrams (CMD) in V and I to a limit of 26 in V. We use the blue, core helium burning stars as a tracer of the star formation rate over the past 600 Myr in both galaxies. While Sextans A shows a relatively high star formation rate during this period, the Pegasus dwarf has been relatively quiescent. We also compare ISM abundances obtained from H II region observations using the Calar Alto 3.5-m telescope. We find that the ISM in the Pegasus dwarf shows a relatively high N/O ratio, while Sextans A shows a relatively low N/O ratio. These results are consistent with the hypothesis that oxygen production is dominated by high mass stars, while nitrogen production is dominated by intermediate to low mass stars. Thus, the star formation history as recorded in the stars is consistent with the star formation history inferred from the ISM abundances.

Key words: **GALAXIES: INDIVIDUAL (SEXTANS A, PEGASUS DIG) — GALAXIES: STELLAR CONTENT — ISM: ABUNDANCES — STARS: FORMATION**

1. SELF-CONSISTENT STAR FORMATION HISTORIES

A long-term goal of extragalactic observational astronomy is to obtain constraints on the star formation histories of galaxies. These constraints can come from observations of the stars or observations of the ISM. When the constraints are in agreement, they merit the label "self-consistent". Here we present some results of self-consistent star formation histories for dwarf irregular galaxies.

Establishing the detailed star formation history of a galaxy is a very difficult task. Two-point star formation histories, like those determined from Hα equivalent widths (Kennicutt 1983; Kennicutt, Tamblyn, & Congdon 1994) give us clues to the question of whether the current star formation rate is comparable to the past average rate, but are unable to answer detailed questions (e.g., was there an early dominant burst of star formation). Gallagher, Hunter, & Tutukov (1984) proposed a three-point scheme based on the dynamical mass, the blue luminosity, and the Hα luminosity, and found that these measures were consistent with roughly constant star formation histories for the irregular galaxies in their sample. Unfortunately, the uncertainties in the conversion of these observables into a star formation history allow consistency with a large range of star formation histories.

Measures of resolved stars offer another avenue. Indeed, there have been many observational programs that have been very successful at modeling the *recent* star formation histories of dIs (e.g., Hodge 1980; Aparicio et al. 1987). However, constraining the *early* star formation histories of galaxies ($\geq$ 1 Gyr) is a very difficult problem. As an example of what can be done from the ground, one can consider the impressive studies of Sextans B (Tosi et al. 1991) and NGC 3109 (Greggio et al. 1993). These galaxies have distance moduli of about 26.6, so with a V-band limit of roughly 23, stars with absolute magnitudes brighter than -3.5 can be reliably recorded. Their method of comparing synthetic color magnitude diagrams (CMDs) to the observations is successful in re-creating the distribution of the stars, but the comparisons are not very sensitive to the star formation histories (i.e., in the upper CMD, the models for constant star formation look very similar to models of exponentially decreasing star formation and models of two distinct bursts). Gallart et al. (1996a,b,c) have pushed this method to its limits (for ground based data) in their study of NGC 6822, and Tolstoy & Saha (1996) have developed a Monte Carlo simulation program which allows them to quantify the errors in their star formation history models, (e.g., Tolstoy 1996).

A significant advance in this field has come about due to the fantastic imaging abilities of the *Hubble Space Telescope*. This has allowed great improvements in the studies of resolved stellar photometry. I will argue that relative chemical abundances can also be used to constrain recent star formation histories. When these two techniques are in agreement, I think that we have achieved self-consistent star formation histories.

2. THE RECENT STAR FORMATION HISTORY OF SEXTANS A

Sextans A is one of four nearby dwarf irregular galaxies observed in a cycle 5 *HST* program to conduct resolved stellar photometry. Program collaborators include Chiosi (Padua), Dufour (Rice), Gallagher, Hoessel (Wisconsin), Mateo (Michigan), Saha (STScI), and Tolstoy (ESA). I will report here some of the results from this study (Dohm-Palmer et al. 1997). The CMD in V and I for Sextans A is shown in the contribution to these proceedings by Dohm-Palmer et al. There we have shown how the superior *HST* photometry allows the "blue plume" to be resolved into two separate populations. There is a well defined main sequence (MS), indicating very recent star formation. Just redward of the main sequence is a clearly separate population that corresponds to massive He-Burning (HeB) stars at the bluest point in their "blue-loop" phase of evolution (e.g., Bertelli et al. 1994; B94). The corresponding red end of this phase can also be seen.

To interpret the recent SFH of Sextans A, we rely upon our knowledge of stellar evolution. There are two main populations which we can use to glean the recent SFH. Traditionally the MS is used, specifically using the strength and position of MS turnoffs. This works very well for isolated generations of stars, such as in clusters. However, the MS in galaxies with continuous star formation can be difficult to interpret because each successive generation lies on top of the previous. We can, however, examine the luminosity function of the MS to look for gaps, flat regions and other features that may give a clue to the SFH (e.g., Butcher 1977). In addition, we can use statistical methods for extracting SFH's from these chronologically over-lapping populations (e.g., Tolstoy & Saha 1996).

The blue HeB stars provide a parallel track to the MS in which to observe star formation events. From the number of stars at each magnitude, we can calculate the SFR for the age corresponding to the time it takes stars to reach this phase of evolution. There are two advantages to using the blue HeB as an indicator of SFH: (1) The blue HeB stars are about 2 mag. brighter than the MS turnoff stars of the same age (e.g., B94). This allows us to probe the recent SFH further back in time (for the same photometric limits) than we can from MS turnoffs; (2) There is little confusion from overlapping generations. All of the blue HeB stars of a certain magnitude come from the same generation of stars (there is confusion from stars leaving the MS, but only at the few percent level). In practice, the blue HeB stars can probe the SFH back to about 600 Myr. At older ages, the blue HeB stars blend with the red clump and horizontal branch, becoming degenerate in time.

To determine the SFH from the MS stars, we analyze the MS in discrete bins. Within each bin, we assume that the mass and the SFR are constant. We also assume the IMF is constant with time. However, each bin will have stars from all generations younger than the turnoff age (TO) for that mass. Thus, we recursively find the SFR by starting with the youngest bin, and work backward through time. One difficulty with this procedure is that the calculated SFR of the oldest bins then depends on that determined for the youngest bins, and in the youngest bins, the counting statistics are low. The errors associated with this, therefore, propagate through the entire SFH determined from the MS. Finally, we convert the rate into units of $M_{\odot}$ Myr^{-1} by multiplying by the average initial mass, which is found by determining the average mass weighted by the IMF. For comparison with other galaxies, we convert the SFR into a SFR/area by dividing by the area covered by the observation (0.92 kpc^2).

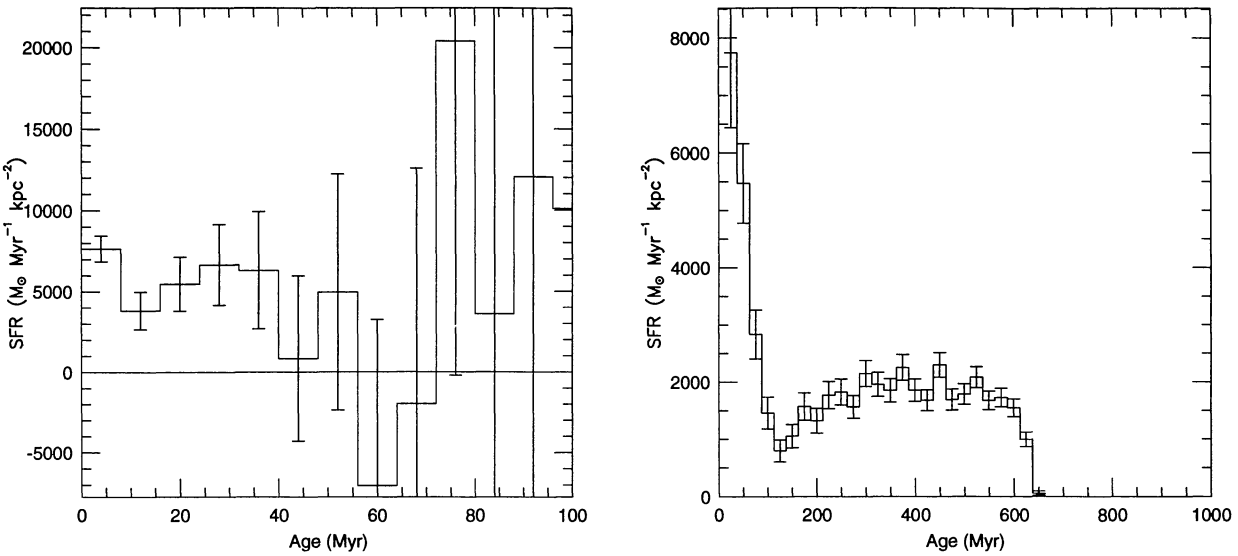

Fig. 1. (left) The global SFR for the area of Sextans A within the field of view determined from the MS luminosity function. A Salpeter IMF has been assumed. This is a result of a recursive process that starts with the youngest bin. The low counts in the youngest bins contribute large uncertainties to all the bins. At several points, the SFR drops below zero, however, within the noise of the counting statistics these are consistent with zero. (right) The SFR for Sextans A over the last 600 Myr, based on the blue HeB stars. The blue HeB luminosity function has been normalized to account for the IMF and the changing lifetime in this phase with mass. Again, a Salpeter IMF has been assumed. For ages older than $\sim$ 600 Myr, there is likely contamination from RGB stars scattering into that region of the CMD. (From Dohm-Palmer et al. 1997)

The MS luminosity function in Sextans A is shown in Dohm-Palmer et al. We have converted the MS luminosity function counts into a SFR as a function of time in Figure 1 (left). We have re-binned the data into linear time bins over the past 100 Myr. Note that at several points the SFR drops below zero. The negative points result from over-subtracting based on the large SFR determined from the youngest bins. This highlights the great difficulty of using the MS to directly determine the SFR when the SFR is relatively constant with time. For the region within the field of view, we see a nearly constant SFR over the past 50 Myr, at $\approx$ 6000 $M_\odot$ Myr^{-1} kpc^{-2} (assuming a Salpeter IMF). Older than 50 Myr, there are large variations in the SFR, but the errors are so large that the rates are consistent with a constant SFR over the past 100 Myr.

Next, we do the same with the blue HeB stars. Again, we analyze the data in discrete bins, and assume that the mass and SFR are constant over these bins. For the blue HeB stars, there are no overlapping generations, and we can assign a single mass and age to each magnitude. The HeB luminosity function of Sextans A (Dohm-Palmer et al., Fig. 2) shows a depressed region at $M_V \sim -4$, between the ages of 80 and 180 Myr. This indicates a quiescent period which was not obvious in the MS luminosity function because our data begins to become incomplete at about the magnitude corresponding to 100 Myr MS turnoff.

The SFR peaks at 50 Myr and then falls a factor of 10 by 120 Myr. It then rises to a nearly constant level near 200 $M_\odot$ Myr^{-1} kpc^{-2} between 200 and 600 Myr. An important caveat is that the field of view covers only a quarter of Sextans A, so the SFH may be quite different outside this field of view.

The resultant SFR is shown in Figure 1 (right). There are four events which are spatially distinct and whose effects can be detected within the field of view (Dohm-Palmer et al. 1997). Note that although we can identify star formation events based on the spatial information, the global SFR appears to be relatively constant over the entire field of view.

3. A COMPARISON WITH THE PEGASUS DWARF IRREGULAR GALAXY

Sextans A can now be contrasted with the Pegasus DIG. The Pegasus dwarf irregular is outstanding for two reasons. First, it is one of the least luminous star forming galaxies in the Local Group with $M_B \approx -12.5$, and second, this system is very gas poor ($\log(M_{\rm H\,I}/L) = -0.53$; Fisher & Tully 1975). VLA H I 21 cm imaging

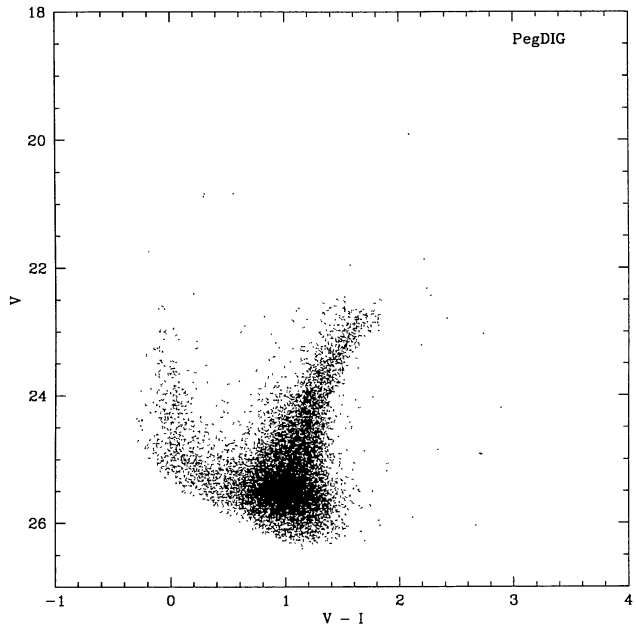

Fig. 2. The CMD in V and I for the Pegaus DIG. The points have been corrected for interstellar reddening. Note the paucity of the MS and HeB populations compared to Sextans A. (From Gallagher et al. 1998, in prep.)

confirmed that the Pegasus dwarf is indeed very gas poor, with both very low H I column density over the entire face of the galaxy and a small H I/optical size ratio (Lo, Sargent, & Young 1993).

Our CMD for Peg DIG is shown in Figure 2. Sextans A and Peg DIG are at very similar distances, so the CMDs have similar photometric limits and covered areas and thus, direct comparisons are possible. The relatively faint MS and the near absence of blue HeB stars shows that while Peg DIG has had some star formation over the last 100 Myrs, the recent star formation rate is clearly depressed relative to that in Sextans A.

This difference can be quantified. In Figure 3, we have constructed the star formation history over the last 600 Myr for the Pegasus dwarf from its HeB stars. Comparing Figure 3 with Figure 1, we see that the average star formation rate in the Pegasus dwarf, over the last 400 Myr, has been roughly about one-tenth that observed in Sextans A.

4. ISM ABUNDANCES AS STAR FORMATION HISTORY CONSTRAINTS

Now lets look at Peg DIG in view of its ISM relative abundances. The discovery of faint, resolved Hα emission through deep narrow-band imaging with the Calar Alto 2.2-m prompted us to propose spectroscopy in order to obtain an ISM abundance (Skillman, Bomans, & Kobulnicky 1997). The brightest H II region is too faint for a direct abundance measurement, but we were able to derive an oxygen abundance of roughly 10% of the solar value from photoionization modeling.

Figure 4 shows the position of Peg DIG in the abundance – luminosity plane in comparison to the well defined sample of dIs assembled by Richer & McCall (1995; RM95). The solid line in Figure 4 is the least squares fit to the more luminous galaxies calculated by RM95 (note that a new distance for Leo A determined from our WFPC2 imaging places it closer to the general trend, Tolstoy et al. in prep.). In Figure 4 it can be seen that Peg DIG fits well in the trend established by other, well studied dwarf irregular galaxies, but lies near the top of the distribution. If the metallicity – luminosity relationship is physically based on a metallicity – mass relationship, then the position of Peg DIG may be due to the lack of recent star formation. This results in a lower blue luminosity per unit mass when compared to more actively star forming galaxies.

Such a scenario is most likely for the lowest mass dwarf galaxies. The higher mass galaxies have, in general, higher metallicities, higher surface brightnesses, and lower gas mass fractions, implying that a current generation of star formation will have a relatively small effect on the present luminosity. However, a burst of star formation can significantly enhance the total luminosity of a dwarf galaxy. Due to the lack of a strong underlying stellar

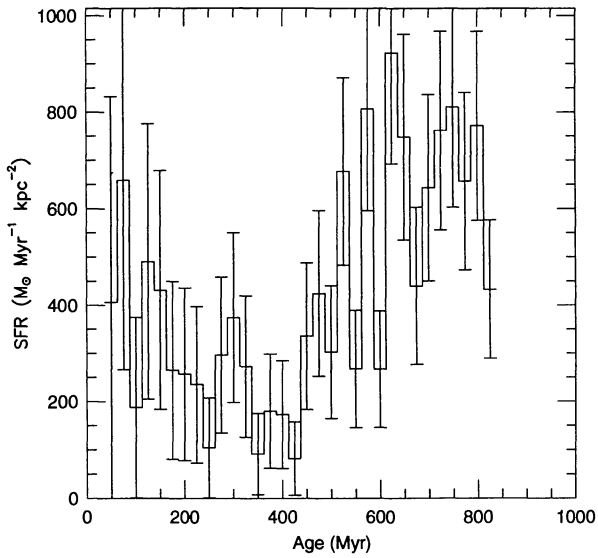

Fig. 3. The SFR for the Pegasus DIG over the last 600 Myr, based on the blue HeB stars. The blue HeB luminosity function has been normalized to account for the IMF and the changing lifetime in this phase with mass. For this plot we used the Salpeter IMF slope. Note the overall lower level of star formation relative to that found in Sextans A. (From Dohm-Palmer et al. 1997)

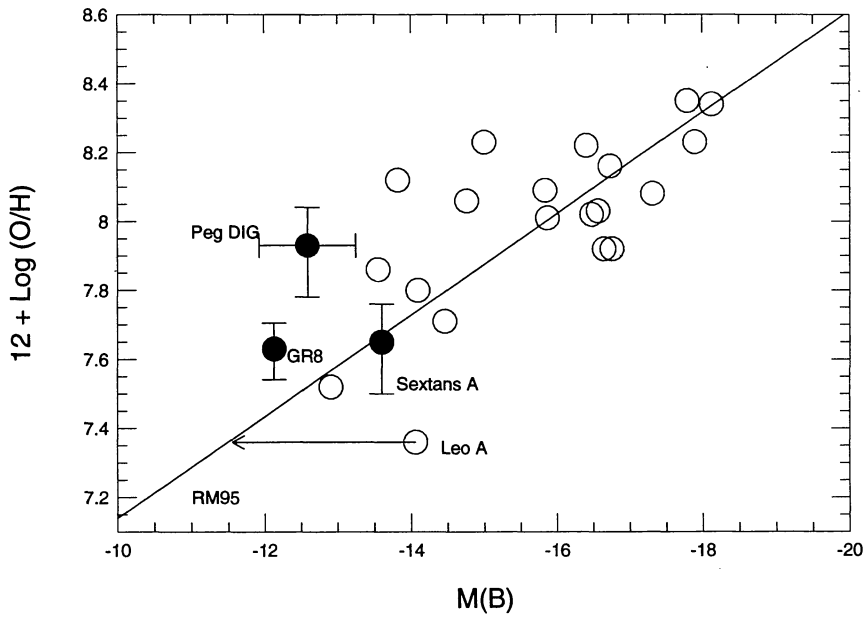

Fig. 4. Plot of H II region oxygen abundance versus absolute blue magnitude following Richer & McCall (1995) (with alterations described in the text). Note the position of Peg DIG. The error bars in oxygen are those implied by the comparison of the observations with photoionization modeling. The new position of Leo A is based on our new WFPC2 CMD.

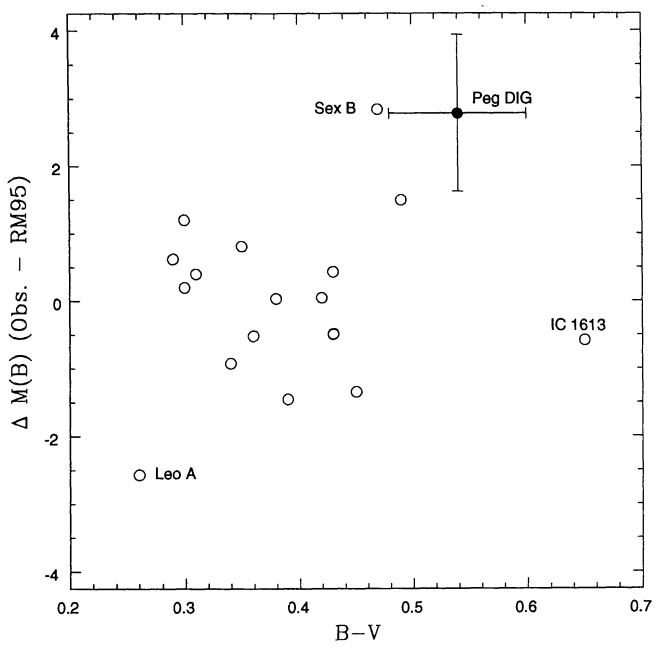

Fig. 5. A comparison of the difference between the observed absolute blue magnitude and that predicted by the metallicity – luminosity relationship as parameterized by RM95 versus the reddening corrected $B-V$ color of the galaxy for the sample of galaxies shown in Figure 4. Peg DIG is seen to be significantly separated from the cluster of points with blue colors and relatively small luminosity differences. Illustrative error bars have been added to the point representing Peg DIG. While no trend is seen in cluster of blue galaxies, we suggest that such a diagnostic diagram (preferably with a longer wavelength difference for the color measurement) may provide a strong test for the origin of the metallicity – luminosity relationship. (From Skillman et al. 1997)

population, as the current burst ages, the fading of an extreme dwarf galaxy will be greatest, thus, leading to a larger scatter in the low luminosity systems (as noted by RM95).

In order to test whether fluctuations in the mass/light ratios of the dIs are the dominant source of the scatter, galaxy colors can be compared versus their positions relative to the mean relationship in the metallicity – luminosity plane. Figure 5 shows such a comparison. Two things are immediately apparent. First, there is a cluster of points with $B-V$ colors between roughly 0.3 and 0.4 with small differences between the predicted and observed blue luminosities (which includes Sextans A). Secondly, Peg DIG lies offset from this group with a redder color and a lower than predicted luminosity. Within the cluster of blue galaxies, there is no evidence for the predicted trend of redder galaxies having fainter luminosities than predicted by the RM95 relationship. However, note that most of the dispersion in the points could be due simply to observational errors (a 0.1 error in log (O/H) translates to an error in the predicted luminosity of 0.7 magnitudes and errors of 0.1 in the color should be typical).

One of the most important features in Figure 5 is the paucity of "reddish" dIs ($B-V \geq 0.5$). This means that there are very few galaxies with which to test the hypothesis. The lack of red dwarf galaxies in the RM95 sample is well understood as a selection effect; observations of bright HII regions are favored for abundance study work. Clearly more abundance studies of red dIs are needed.

Since the metallicity of Peg DIG appears to make sense, lets check on the relative abundances. Figure 6 shows the N/O abundances versus O/H for the sample of dIs and HII galaxies compiled by Kobulnicky & Skillman (1996). Only the points for those galaxies which do not show evidence of WR features in their spectra are plotted. Peg DIG stands at the upper envelope of the values of N/O. Recent Calar Alto observations of Sextans A have allowed us to determine an N/O (Skillman, et al. in prep.), and note that Sextans A appears near the lower envelope of values.

Kobulnicky & Skillman (1996, 1997) have argued that ISM abundances mainly reflect the past chemical enrichment history and not current "pollution". In this interpretation, it may be possible to see depressed values of N/O in galaxies which have had recent episodes of star formation (O production happens quickly in

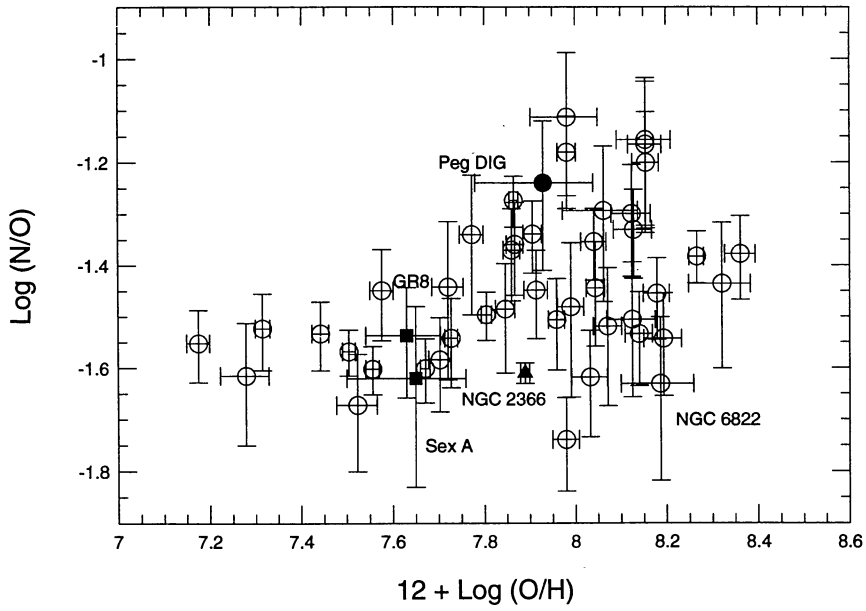

Fig. 6. A comparison of the N/O and O/H in Peg DIG with the collection of dwarf irregular galaxies and H II galaxies assembled by Kobulnicky & Skillman (1996; see their Table 5 and Figure 15 for identification of individual points). Only galaxies without WR emission features and errors in log (N/O) less than 0.2 have been plotted. Note the positions of Peg DIG and Sextans A.

massive star and is over within a few tens of millions of years while N enrichment is delayed because it forms in more slowly evolving intermediate mass stars with ages in excess of 100 Myr). On the other hand, in galaxies that have been relatively quiescent for a long period of time one would expect relatively high values of N/O (Edmunds & Pagel 1978).

The positions of Peg DIG and Sextans A in Figure 6, and their recent star formation histories as recorded in their CMDs appear to support this simple picture. Maintaining some skepticism, I could point out that there is a smaller range in N/O at the very low metallicity end of the scale, and, thus, maybe the position of Sextans A is not telling us that much. However, I return to my point that there are very few abundance studies on quiescent or reddish dIs. If we can study some of these systems at low metallicity, we may turn up some higher values of N/O (but note that these are not predicted in the simple scheme of nitrogen production being chiefly primary at low metallicity).

At this time, it is not possible to compile an extensive list of objects to test this hypothesis, but there are some other important test cases worth mentioning. NGC 6822 has one of the lowest values of N/O (log (N/O) = −1.66; Pagel, Edmunds, & Smith 1980). In NGC 6822, Hodge (1980) found evidence for stellar cluster formation over the last 100 Myr, with a strongly enhanced period of stellar cluster formation in the interval 75 to 100 Myr ago. Marconi et al. (1995) found evidence for episodic star formation in NGC 6822, but the resolution of their modeling does not allow for a precise star formation history over the last few 100 Myr. Gallart et al. (1996c) found an enhancement in the star formation rate over the last 100–200 Myr. If the stellar cluster formation history reflects the overall star formation history, then it appears that NGC 6822 has experienced a productive period of star formation over the last 50 – 200 Myr, which has not yet resulted in the elevation of the ISM N abundance. This could be consistent with N production delayed by a few 100 Myr.

Finally, we consider the case of NGC 2366. This galaxy currently shows a relatively high rate of massive star formation as evidenced by its Hα/L(B) ratio (Hunter, Hawley, & Gallagher 1993). Aparicio et al. (1995) present evidence for a dominant burst of star formation roughly 20 – 50 million years ago. On the other hand, based on deeper photometry, Tolstoy (1995) finds a relatively constant star formation rate over the last 300 million years. Although it is important to sort out this discrepancy, both studies support the view of vigorous star formation during the last few hundred million years in NGC 2366. This may be consistent with the relatively low N/O observed (log (N/O) = −1.61; González-Delgado et al. 1994).

In the future, with deeper stellar photometry (using *HST*) and statistical treatment of CMDs like those presented by Greggio (1994), Tolstoy (1995), and Aparicio et al. (1996), it should be possible to determine much more accurate star formation histories for the last 1 Gyr for a large sample of the nearby dIs. If the preliminary evidence presented here for delayed N production holds up, then it should be possible, in principle, to calibrate the length of that delay. This would be of great value in understanding the chemical evolution of galaxies. For example, Pettini, Lipman, & Hunstead (1995) and Lipman (1995) find very low values for log (N/O) of ~ -2 for several damped Lyman-α system of low metallicity. They favor an interpretation of delayed N production which means that they are observing these systems within a few hundred million years of dominant star formation episodes. Since the nearby dIs have similar metallicities to these damped Lyman-α systems, it is reasonable to expect that the stellar populations are similar. Thus, more studies of the nearby dIs can help us to understand galaxy formation at redshifts of 2 to 3 seen in the damped Lyman-α systems.

REFERENCES

Aparicio, A. et al., 1995, AJ, 110, 212
Aparicio, A., Gallart, C., Chiosi, C., & Bertelli, G. 1996, ApJ, 469, L97
Aparicio, A., Garcia-Pelayo, J. M., Moles, M., & Melnick, J. 1987, A&AS, 71, 297
Bertelli, G., Bressan, A., Chiosi, C., Fagotto, F. & Nasi, E. 1994, A&AS 106, 275, (B94)
Butcher, H. 1977, ApJ, 216, 372
Dohm-Palmer, R. C., Skillman, E. D., Saha, A., Tolstoy, E., Mateo, M., Gallagher, J., Hoessel, J., & Dufour, R. J. 1997, AJ, submitted
Edmunds, M. G., & Pagel, B. E. J. 1978, MNRAS, 185, 78
Fisher, J. R., & Tully, R. B. 1975, A&A, 44, 151
Gallagher, J. S., Hunter, D. A., & Tutukov, A. V. 1984, ApJ, 284, 544
Gallart, C., Aparicio, A., & Víchez, J. M. 1996a, AJ, 112, 1928
_____. 1996b, AJ, 112, 1950
Gallart, C., Aparicio, A., Bertelli, G., & Chiosi, C. 1996c, AJ 112, 2596
Gonzalez-Delgado, R. M. et al., 1994, ApJ, 437, 239
Greggio, L. 1994, in The Local Group: Comparative and Global Properties, ed. A. Layden, R. C. Smith, & J. Storm) ESO, p. 72
Greggio, L., Marconi, G., Tosi, M., & Focardi, P. 1993, AJ, 105, 894
Hodge, P. W. 1980, ApJ, 241, 125
Hunter, D. A., Hawley, W. N., & Gallagher, J. S. 1993, AJ, 106, 1797
Kennicutt, R. C., Jr. 1983, AJ, 88, 483
Kennicutt, R. C., Jr., Tamblyn, P., & Congdon, C. W. 1994, ApJ, 435, 22
Kobulnicky, H. A., & Skillman, E. D. 1996, ApJ, 471, 211
_____. 1997, ApJ, in press
Lipman, K. 1995, Ph.D. Thesis, Cambridge University
Lo, K. Y., Sargent, W. L. W., & Young, K. 1993, AJ, 106, 507
Marconi, G., Tosi, M., Greggio, L., & Focardi, P. 1995, AJ, 109, 173
Pagel, B. E. J., Edmunds, M. G., & Smith, G. 1980, MNRAS, 193, 219
Pettini, M., Lipman, K., & Hunstead, R. W. 1995, ApJ, 451, 100
Richer, M. G., & McCall, M. L. 1995, ApJ, 445, 642, (RM95)
Skillman, E. D., Bomans, D. J., & Kobulnicky, H. A. 1997, ApJ, 474, 205
Tolstoy, E. 1995, Ph.D. Thesis, University of Groningen
_____. 1996, ApJ, 462, 684
Tolstoy, E., & Saha, A. 1996, ApJ, 462, 672
Tosi, M. Greggio, L., Marconi, G., & Focardi, P. 1991, AJ 102, 951